Quantile ARDL Estimation of the Relationship between Confirmed COVID-19 Cases and Deaths in the U.S.

XIN JING
Department of Trade and Economics, Anhui Xinhua University, Hefei, Anhui 230088, China
Email: superheunheun@gmail.com

JIN SEO CHO
School of Economics, Yonsei University, Seodaemun-gu, Seoul 03722, Korea
Email: jinseocho@yonsei.ac.kr

This version: March 25, 2026

Abstract

This study uses the quantile ARDL methodology to examine the dynamic link between confirmed COVID-19 cases and deaths in the U.S. after vaccination, with a particular emphasis on exploring heterogeneity across various percentiles. The findings indicate that the confirmed case fatality rate decreased after vaccination, and the relationship between confirmed cases and deaths varies across different percentiles.

Key Words: Quantile ARDL; Cointegration; COVID-19; Vaccination; Heterogeneity.

JEL Classifications: C12, C22, I18.

Acknowledgements: The editor, Jinill Kim, and two anonymous referees provided very helpful comments for which we are most grateful. Jing acknowledges financial support from the Department of Education of Anhui Province, China (2025AHGXSK40043), and Cho acknowledges Chang-am fellowship and financial support from the Ministry of Education of the Republic of Korea and the National Research Foundation of Korea (NRF-2020S1A5A2A01040235).

1 Introduction

Since the start of the COVID-19 pandemic, numerous countries worldwide have enforced strict measures to contain the virus's spread, and these measures have also entailed substantial economic expenses, leading to previously unseen financial losses (Forsythe et al., 2020; Deb et al., 2022b).

Vaccination campaigns have had a substantial positive impact on economic recovery from a health economics perspective (Utami et al., 2023; Hansen and Mano, 2023) and have also been highly effective in reducing confirmed cases and deaths.

However, hesitancy and refusal to be vaccinated continue to undermine the effectiveness of these interventions. Pandemic control efforts can be undermined by vaccine hesitancy and refusal, which also have significant impacts on the global economy (e.g., Rawlings et al., 2022). Annual productivity losses due to unvaccinated workers are estimated to be around USD 15 billion, even though vaccinations have already lowered COVID-related costs by approximately 80% (see Padula et al., 2021). In addition to the economic consequences, vaccine hesitancy and refusal exhibit substantial heterogeneity. For example, Goel et al. (2023) demonstrate that US states with higher wealth, a larger elderly population, and more physicians tend to have lower levels of vaccine hesitancy (e.g., Kountouris and Remoundou, 2024; Tan et al., 2022; McPhedran and Toombs, 2021). Furthermore, vaccine hesitancy is associated with educational attainment, age, vaccine characteristics, vaccination methods, and media coverage (e.g., Kountouris and Remoundou, 2024; Tan et al., 2022; McPhedran and Toombs, 2021). Overall, these findings indicate that both the pandemic and the vaccination campaign have affected the population in heterogeneous ways.

In the current study, we focus on the fatality rate of COVID-19 that associates confirmed cases with deaths and empirically examine how the rate is formed heterogeneously while considering the vaccination effect. For this purpose, we characterize the underlying heterogeneity using the conditional quantiles of the death distribution and next employ the Quantile Autoregressive Distributed Lag (QARDL) methodology proposed by Cho et al. (2015) to estimate the effect of distributional heterogeneity.

The analysis of the fatality rate considering distributional heterogeneity remains relatively scarce in the literature. Ullah et al. (2022) note significant differences exist in the number of confirmed cases and deaths across the US states, providing valuable insights into asymmetric economic activities. Mehta et al. (2023) and Chang et al. (2023) also apply the Autoregressive Distributed-Lag (ARDL) methodology to analyze the impact of COVID-19 on real estate, food, and healthcare industries. Nevertheless, the existing studies pay little attention to heterogeneity in fatality rates, although accommodating its existence provides analysis outcomes distinct from assuming homogeneity.

QARDL is useful for detecting distributional heterogeneity in fatality rates and examining the effects of vaccination. Furthermore, the currently available COVID-19 data often contain noise, outliers, biases, skewness, and truncation issues (e.g., Jing and Cho, 2025). However, quantile regression is robust in handling outliers and capturing heterogeneity as Jiang et al. (2022) demonstrate by focusing on the short-term forecasts of the confirmed cases. Given that QARDL applies quantile regression to nonstationary series, its useful features are exploited to estimate the fatality rate defined as the long-run relationship between confirmed cases and deaths.

The current study contributes to the literature by applying QARDL to COVID-19 data as follows. First, we provide a novel quantile-based analysis of the COVID-19 fatality rate by explicitly modeling the heterogeneous long- and short-run dynamics between confirmed cases and deaths. Unlike existing studies that rely primarily on mean-based frameworks, our approach reveals distributional heterogeneity in the fatality rate across different conditional quantiles. Second, we incorporate vaccination effects into the QARDL framework, offering new empirical evidence on how large-scale vaccination campaigns shape the dynamic relationship between infection and fatality across different regions of the conditional distribution. Third, the QARDL methodology enables us to capture nonlinearity, persistence, and heterogeneity in nonstationary time series. Using this feature, we extend the application of quantile-based time-series analysis to health economics and epidemiology literature.

The remainder of this paper is organized as follows. Section 2 provides a comprehensive literature review that forms the basis and motivation of this study. Section 3 details the QARDL estimation methodology, highlighting its theoretical framework and advantages over conventional approaches. Section 4 presents the empirical analysis of the dynamic relationship between confirmed COVID-19 cases and deaths across different percentiles. Finally, Section 5 summarizes the key findings, discusses their policy implications, and outlines directions for future research.

2 Literature Review

An increasing number of studies have examined infection and death counts during the COVID-19 pandemic during the global health crisis. These studies help understand the mechanisms of viral transmission and fatality and offer valuable guidance for public health policymaking. This dynamic relationship evolves as vaccination coverage continues to expand. Further investigation into the potential heterogeneity under widespread vaccination is warranted. Drawing on the existing literature, we discuss the determinants of COVID-19 fatality, the role of vaccination, recent findings on the dynamic case-fatality relationship, and the

latest methodological advances for empirical analysis in this section.

Existing studies have shown that multiple factors influence COVID-19 fatality. First, demographic characteristics, such as age and gender, play a decisive role in fatality differences (e.g., Verity et al., 2020; Torres et al., 2023; O'Driscoll et al., 2021). Second, underlying chronic conditions, such as hypertension, diabetes, and cardiovascular diseases, significantly increase the risk of death (e.g., Lee and Hwang, 2025). In addition, the adequacy of medical resources, such as the number of general practitioners and hospital beds per capita, as well as government interventions, including lockdown policies, social distancing, and travel restrictions, also have important effects on fatality (e.g., Di Porto et al., 2022; Fang et al., 2020).

Widespread vaccination is a crucial pandemic control measure. Multiple empirical studies have demonstrated that vaccines significantly reduce infection and severe illness rates, thereby indirectly lowering fatality (e.g., Kim and Lee, 2022). However, vaccine effectiveness exhibits spatial and population heterogeneity, as elderly individuals, immunocompromised patients, and viral variants may affect vaccine efficacy (e.g., Tiu et al., 2022; Mori et al., 2023). Some studies have also suggested that the protective efficacy of vaccines may gradually decline over time following vaccination (e.g., Suah et al., 2022).

Existing studies suggest a dynamic lag relationship between confirmed cases and deaths (e.g., Jin, 2021). Some studies employ time series models to forecast and analyze the number of confirmed COVID-19 cases and deaths (e.g., Liu et al., 2021; Gupta and Pal, 2020; Sujath et al., 2020). Due to its favorable properties in small samples, the traditional ARDL model has been widely applied in COVID-19 pandemic analysis (e.g., Chang et al., 2023; Jeris and Nath, 2020). However, the ARDL model assumes homogeneity in the relationships between variables across all levels, which fails to capture the influence of heterogeneity on fatality rate under different severity conditions.

In recent years, quantile regression has been widely applied in health research to reveal heterogeneous effects across different regions of distribution (e.g., Okada, 2018; Chen et al., 2016; Silva et al., 2018). In the context of COVID-19 research, quantile regression methodology can detect heterogeneous relationships between confirmed cases and deaths across different regions of the conditional distribution, particularly capturing the dynamic features at extreme values, such as the observations belonging to the upper tail region of death distribution (e.g., Jiang et al., 2022; Ribeiro et al., 2021).

The QARDL model combines ARDL's dynamic properties with quantile regression to identify heterogeneity, allowing for short- and long-run dynamics estimation across different percentiles. In the fields of macroeconomics and finance, QARDL has been popular in effectively capturing nonlinearity and distributional heterogeneity (e.g., Cho et al., 2015; Hammoudeh et al., 2022; Hashmi et al., 2022). However, its application in health economics remains relatively new, particularly in the analysis of COVID-19 data.

Overall, although the determinants of COVID-19 fatality and the effectiveness of vaccination have been extensively examined in the existing literature, systematic empirical evidence on the existence of quantile-dependent dynamic differences between confirmed cases and deaths in the post-vaccination period is lacking. This study employs the QARDL methodology to analyze the dynamic relationship between confirmed cases and deaths across different percentiles in the context of vaccination in the United States, providing more nuanced evidence for understanding the evolution of the pandemic and offering new empirical insights for public health policymaking.

3 QARDL Estimation and Inference

Cho et al. (2015) extend the ARDL approach by applying quantile regression and jointly analyzing the short- and long-run relationships across a range of percentiles, which is known as the QARDL methodology. This section applies the QARDL methodology to the COVID-19 data environment.

The QARDL methodology assumes different cointegrating coefficients depending on the percentile. Specifically, it assumes the following relationship:

$$Y_t = \alpha_*(\tau) + \sum_{j=1}^{p} \phi_{j*}(\tau) Y_{t-j} + \sum_{j=0}^{q} \boldsymbol{\theta}_{j*}(\tau)' \mathbf{X}_{t-j} + U_t(\tau).$$

This specification is commonly referred to as QARDL(p, q) process. Here, $\Delta \mathbf{X}_t$ is assumed to be a k-dimensional stationary ergodic process ($k \in \mathbb{N}$); the error term $U_t(\tau)$ is defined as $Y_t - Q_\tau(Y_t|\mathcal{F}_{t-1})$, where $Q_\tau(Y_t|\mathcal{F}_{t-1})$ is the conditional quantile function on $\mathcal{F}_{t-1}$; $\mathcal{F}_{t-1}$ is the smallest σ-field generated by $\{\mathbf{X}_t', Y_{t-1}, \mathbf{X}_{t-1}', \ldots\}$; and p and q are the QARDL lag orders such that $U_t(\tau)$ is identically and independently distributed.

Based on the existing empirical and theoretical analyses, current deaths D_t and confirmed cases C_t are cointegrated. That is, a long-run relationship exists between confirmed cases and deaths, which is represented as

$$D_t = \beta_* C_t + \varepsilon_t,$$

where β_* denotes the long-run fatality rate (e.g., Brodeur et al., 2021). Here, ε_t represents the cointegration error. If ε_t is stationary, the QARDL process is rewritten as follows:

$$\triangle D_t = \alpha_* + \zeta_* D_{t-1} + \gamma_* C_{t-1} + \sum_{j=1}^{p-1} \lambda_{j*} \triangle D_{t-j} + \sum_{j=0}^{q-1} \delta_{j*} \triangle C_{t-j} + U_t$$

such that U_t is identically and independently distributed, which is ensured by letting the lag orders p and q be sufficiently large. By substituting the cointegrating relationship $D_{t-1} = \beta_* C_{t-1} + \varepsilon_{t-1}$, we obtain the following ARDL(p, q) process:

$$\triangle D_t = \alpha_* + \zeta_*(D_{t-1} - \beta_* C_{t-1}) + \sum_{j=1}^{p-1} \lambda_{j*} \triangle D_{t-j} + \sum_{j=0}^{q-1} \delta_{j*} \triangle C_{t-j} + U_t \tag{1}$$

where $\beta_* := -\frac{\gamma_*}{\zeta_*}$.

Each parameter in (1) has the following interpretations. First, the Error Correction Model (ECM) parameter ζ_* measures the smoothing fatality that reflects the adjustment speed of deaths toward the long-run equilibrium with confirmed cases. Second, the long-run cointegration coefficient β_* measures the fatality rate. Third, the momentum effect of death growth $\lambda_* := \sum_{j=1}^{p-1} \lambda_{j*}$ measures the cumulative impact of the lagged changes in D_t on the current deaths, viz., $\sum_{j=1}^{p-1} \partial \triangle D_t / \partial \triangle D_{t-j}$. Finally, the impulse response coefficient of the death change to the newly confirmed cases, viz., $\delta_* := \sum_{j=0}^{q-1} \delta_{j*}$, assesses the impact of the most recent changes in confirmed cases on the current death change. Note that δ_* measures the short-run impact of the change in newly confirmed cases on the change in deaths. It accounts for the effect of multiple lags, whereas β_* describes the relationship between the number of newly confirmed cases and deaths, reflecting the pandemic's long-run fatality rate. In short, δ_* focuses on the short-run dynamic adjustment, while β_* represents the pandemic's long-run fatality rate.

The signs of some parameters are predetermined based on their definitions. First, $-1 < \zeta_* < 0$ is implied by the long-run relationship between C_t and D_t. A significant and negative coefficient implies a strong corrective force toward the long-run equilibrium. Second, $0 < \beta_* < 1$ is implied by the long-run relationship. By definition, the long-run relationship between C_t and D_t is neither negative nor greater than unity.

We extend the ARDL expression to QARDL specification and allow for heterogeneous relationships between confirmed cases and deaths. For each percentile $\tau \in (0, 1)$, the following is the QARDL(p, q) model:

$$\triangle D_t = \alpha_*(\tau) + \zeta_*(\tau)(D_{t-1} - \beta_*(\tau) C_{t-1}) + \sum_{j=1}^{p-1} \lambda_{j*}(\tau) \triangle D_{t-j} + \sum_{j=0}^{q-1} \delta_{j*}(\tau) \triangle C_{t-j} + U_t(\tau). \tag{2}$$

This specification allows the coefficients in (1) to differ from those of different percentiles so that heterogeneous cointegrating relationships exist between D_t and C_t. Here, the percentile τ represents the different location of the conditional distribution of deaths on the past information, which can differ from explicitly de-

fined population groups or individual-level mortality risk. Accordingly, QARDL captures the distributional heterogeneity in deaths over time.

Although the quantile-specific estimates do not explicitly identify the underlying sources of heterogeneity, they reflect the differences across the regions of conditional death distribution. Higher percentiles correspond to observations in which death is highly likely to occur within the conditional distribution. Meanwhile, lower percentiles correspond to observations with relatively fewer deaths. As Ullah et al. (2022) highlight, significant differences exist in the projections of confirmed COVID-19 cases and deaths across the US states. (see also Deb et al., 2022a; Hansen and Mano, 2023). This suggests potential systematic variations in the fatality rate, leading to the existence of heterogeneous relationships across the regiosn of conditional death distribution. The QARDL model in (2) characterizes heterogeneity in terms of distributional differences in deaths.

To detect heterogeneous relationships, the Wald test principle is applied to the estimated coefficients. Specifically, we test for different relationships between confirmed cases and deaths across percentiles. The following four null hypotheses are considered:

$$H_0^{\zeta} : \zeta_*(0.25) = \zeta_*(0.5) = \zeta_*(0.75), \qquad H_0^{\beta} : \beta_*(0.25) = \beta_*(0.5) = \beta_*(0.75),$$

$$H_0^{\lambda} : \lambda_*(0.25) = \lambda_*(0.5) = \lambda_*(0.75), \qquad H_0^{\delta} : \delta_*(0.25) = \delta_*(0.5) = \delta_*(0.75).$$

The heterogeneous relationship provides valuable policy implications. For example, strategically developed control measures can be implemented to efficiently curb the spread of the virus to the extent of heterogeneity. As another example, the vaccination campaign can result in different consequences depending on the heterogeneity.

4 Empirical Analysis

In this section, we conduct the empirical analysis by applying the QARDL methodology to the empirical data in the United States.

First, we describe the data used in this study. The US COVID-19 confirmed case and death data are obtained from the World Health Organization's Coronavirus Dashboard.[1] Given the crucial role of vaccination in the pandemic progress, we explicitly incorporate the timing of vaccine administration into our sample selection. The first COVID-19 vaccine dose was administered on December 8, 2020 outside of clinical trials.

[1]The data are available at the following URL: https://ourworldindata.org/covid-vaccinations.

As of December 8, 2021, approximately 55.9% of the global population received at least one dose; 45.5% completed two doses; and 4.3% received booster shots.

The sample period is from December 8, 2020, to December 7, 2021. This sample period enables us to analyze the dynamic relationship between confirmed cases and deaths in the context of large-scale vaccination efforts. All daily observations are collected to capture the fluctuations and potential dynamic features between the two variables.

A preliminary empirical analysis is conducted before the empirical estimation results are discussed. First, Table 1 reports the descriptive statistics of daily new confirmed COVID-19 cases and deaths per million population in the United States over the sample period. The average number of daily new confirmed cases is 276.17 per million, with a substantially dispersed distribution as reflected by the standard deviation of 188.50 and a wide range between the minimum (24.46) and maximum (863.48) values. Similarly, daily deaths per million exhibit noticeable variation. The mean and standard deviation are 4.00 and 3.01, respectively. The positive skewness and excess kurtosis in both series indicate extreme observations and heavy-tailed distributions, highlighting pronounced non-normality and heterogeneity of the data. This motivates the use of the QARDL framework. Second, we apply the Augmented Dickey-Fuller (ADF) unit root test to the same data under four specifications: with and without a deterministic trend, and for both level and first-differenced series. Table 2 reports the results. The null hypothesis of a unit root cannot be rejected at levels for both confirmed cases and deaths, indicating non-stationarity in levels. However, after first differencing, the null hypothesis is strongly rejected at the 1% significance level in all cases. These results suggest that both variables are integrated of order one, I(1), thereby satisfying the integration requirements for applying the QARDL methodology.

<Insert Tables 1 and 2 around here>

4.1 Full Sample Analysis

Here, we report the results of QARDL estimation based on the full sample. The lag orders are set to $p = 7$ and $q = 2$ according to the Bayesian information criterion (BIC). As shown in Table 3, the estimated coefficients are statistically significant across all percentiles, indicating the robustness of the model specification and the existence of heterogeneous dynamic relationships across different percentile levels.

To better illustrate the quantile-dependent effects, we plot the estimation results in Figure 1. The figure presents the estimated trajectories of the four key parameters: $\zeta_*(\tau)$, $\beta_*(\tau)$, $\lambda_*(\tau)$, and $\delta_*(\tau)$ across the percentiles ranging from 0.1 to 0.9. We also provide the 90% confidence bands of the estimated parameters

to assess the precision and statistical significance of the estimates at each percentile.

<Insert Figure 1 and Table 3 around here>

The quantile-specific coefficient estimates reveal clear evidence of location asymmetry, indicating that the dynamic relationship between confirmed cases and deaths systematically varies across different regions of the conditional death distribution. The heterogeneous effects captured by the QARDL model highlight that the distributional effect produces different estimates for different percentiles, which is often overlooked in conventional mean-based model estimation.

The estimation results are summarized as follows. First, the ECM parameter $|\zeta_*(\tau)|$ indicates a clear downward trend in the adjustment speed for the increase in the percentile level. Specifically, at lower percentiles (e.g., $\tau = 0.1$), the adjustment speed reaches as high as 33.2%, implying that the system corrects deviations from the long-run equilibrium at a relatively faster pace. This suggests that short-term fluctuations in the relationship between confirmed cases and deaths are more easily absorbed and stabilized at lower conditional quantiles of deaths. In contrast, at higher percentiles (e.g., $\tau = 0.9$), the estimated adjustment speed drops sharply to 7.6%, indicating that the convergence to the long-run equilibrium is substantially slower. This slower adjustment process reflects the fact that factors such as overloaded healthcare system, shortage of medical resources, delays in reporting, and increasing uncertainty regarding treatment effectiveness may contribute to the prolonged deviation from the equilibrium. Based on this finding, we conclude that the heterogeneity in adjustment speed across different percentiles contributes to the joint distribution between confirmed cases and deaths.

Second, the estimation results of the fatality rate $\beta_*(\tau)$ reveal a clear upward trend for the increase in the percentile level, indicating another significant heterogeneity across different percentiles. At lower percentile levels (e.g., $\tau = 0.1$), the estimated fatality rate is relatively low, with $\beta(\tau) = 0.01$, suggesting that the proportion of deaths relative to confirmed cases remains small. This is consistent with the relatively lower number of deaths at lower conditional quantiles of deaths, which may reflect, on average, more favorable epidemiological and healthcare conditions. In contrast, at higher percentile levels (e.g., $\tau = 0.9$), the fatality rate rises sharply to 0.04, indicating that the death count increases substantially relative to confirmed cases. This sharp rise can be attributed to overwhelmed healthcare systems, the shortage of intensive care resources, or a higher proportion of vulnerable groups, such as the elderly and individuals with pre-existing medical conditions. These findings further support the view of Ullah et al. (2022) that significant variations in COVID-19 fatality rates exist in the United States, and our model effectively captures this feature through the heterogeneity characterized by the conditional distribution of deaths.

Third, the estimation results of the momentum parameter $\lambda_*(\tau)$ show a decreasing trend for the increase in the percentile level, declining from -2.27 at $\tau = 0.1$ to -3.60 at $\tau = 0.9$. This pattern indicates that the momentum effect is more escalated at higher percentiles. Specifically, the increasingly negative value of $\lambda_*(\tau)$ suggests that past deaths exert a stronger suppressive effect on current deaths as the pandemic intensifies. A weaker moment parameter is estimated at lower percentile levels with lower death conditional quantile. The weaker momentum effect implies that past values have less influence on current deaths. In contrast, the momentum effect becomes more pronounced at higher percentile levels, indicating that past deaths have a stronger dampening impact on current deaths.

Fourth, the estimated response coefficient $\delta_*(\tau)$ fluctuates between 0.008 and 0.01 across all percentiles. This indicates that a short-run fluctuation in confirmed cases has a positive impact on the change in deaths. This result highlights that even low levels of variation in confirmed cases affect the short-term death count.

Finally, we conduct parameter heterogeneity tests across different percentiles. In the bottom panel of Table 3, we report the Wald test statistics for the null hypotheses described in Section 3. The test results strongly reject the null hypotheses for $\zeta_*(\tau)$, $\beta_*(\tau)$, and $\lambda_*(\tau)$, indicating that the parameters exhibit significant heterogeneity across different percentiles. This implies that the speed of error correction, fatality rate, and momentum effect substantially vary with pandemic severity. This further highlights the importance of incorporating quantile-dependent dynamics in the relationship between confirmed cases and deaths. In contrast, the test for $\delta_*(\tau)$ fails to reject the null hypothesis, suggesting that the short-run dynamics captured by $\delta_*(\tau)$ does not show a significant variation across different percentiles.

4.2 Sub-Sample Analysis

In this section, we examine the impact of the vaccination campaign on the parameters across different percentiles over different sample periods.

First, we clarify the objective of the sub-sample analysis, which is distinctive from the full-sample analysis. The full-sample estimation aims to capture the average quantile-dependent dynamic relationship between confirmed cases and deaths over the entire sample period. In contrast, we conduct a sub-sample analysis to examine whether this relationship evolves in response to the vaccination rollout and the changing pandemic conditions. We can assess the temporal stability of the QARDL estimates and identify potential structural changes that may not be evident from the full-sample analysis by allowing the model parameters to possibly differ across rolling sub-samples.

To this end, we first plot the estimates of the four parameters. Figure 2 shows the estimates obtained using observations in numerous samples along with their 90% confidence bands. A robust rolling estimation

technique with a window length of 266 days is employed to ensure sufficient observations. Specifically, the rolling window approach shifts the sample window forward one day at a time until the end of the sample period is reached. This approach enables us to dynamically track the evolution of parameter estimates in response to pandemic and vaccination changes. As shown in Figure 2, the rolling quantile regression estimates display pronounced time-varying patterns across different percentile levels. This indicates that the relationship between confirmed cases and deaths is not only heterogeneous across percentiles but also dynamically evolves.

<Insert Figure 2 around here>

We specifically examine the parameters estimated. First, the estimated degree of smoothing fatality $|\zeta_*(\tau)|$ decreases as the percentile increases throughout the entire period. Location asymmetry is relatively strong in the early period, with the average adjustment speed being approximately 22.0%, 14.0%, and 12.0% for $\tau = 0.25$, $\tau = 0.5$, and $\tau = 0.75$, respectively. In the middle period, the location asymmetry peaks at 30.0%, 20.0%, and 10.0%, respectively. However, the location asymmetry weakens in the later period. All the estimated values are about 20% for all percentiles. The United States began its vaccination campaign in December 2020 and accelerated its schedule in the spring of 2021. A broad vaccination infrastructure was established during the first few months of the year, which led to significant changes in the parameter estimates from December 02, 2021 to April 11, 2021.

Second, the rolling quantile regression estimates of $\beta_*(\tau)$ show a clear downward trend, indicating a significant decrease in the fatality rate after the vaccination campaign began. Although vaccination is not explicitly included as an explanatory variable in the empirical model, the observed time variation in the estimated parameters coincides closely with the vaccination rollout period. Therefore, this result may show the systematic change in the case-fatality relationship associated with the vaccination phase, although it may not strictly describe the causal effect. In addition, $\beta_*(\tau)$ exhibits significant location asymmetry throughout the entire period, such that the estimated $\beta_*(\tau)$ increases as τ increases. In the early period, the fatality rate is approximately estimated as 1.20%, 1.70%, and 2.20% for $\tau = 0.25$, $\tau = 0.5$, and $\tau = 0.75$, respectively. However, these estimated rates drop to 1.10%, 1.40%, and 1.80% over time, respectively. The decline in fatality rate is more pronounced at higher percentiles. That is, the vaccination has exerted a stronger effect at higher conditional death quantiles.

Third, the momentum effect of the death change exhibits a location asymmetry in the later period, with $\lambda_*(\tau)$ being -3.0, -3.5, and -4.0 at $\tau = 0.25$, $\tau = 0.5$, and $\tau = 0.75$, respectively. In contrast, the rolling quantile regression estimates of $\zeta_*(\tau)$ remain stable at approximately 0.005 throughout the entire sample

period.

Finally, the p-values of the Wald tests are presented based on the rolling estimates in Figure 3. The results show that the null hypotheses of parameter constancy for $\zeta(\tau)$ and $\beta(\tau)$ are strongly rejected throughout the entire sample period, indicating that both the error correction speed and fatality rate exhibit persistent heterogeneity over time and across different percentiles. This suggests that even under continuous vaccination progress, both the adjustment process toward long-run equilibrium and the fatality dynamics remain highly sensitive to pandemic conditions. However, the location asymmetry of $\lambda_*(\tau)$ is statistically significant only in the later sample period. This finding reflects that the dynamic feedback between past and current deaths becomes increasingly complex and asymmetric as the pandemic evolves. In contrast, the test results for $\zeta_*(\tau)$ indicate that its location asymmetry is not statistically significant throughout the entire period, suggesting a relatively stable behavior over time.

<Insert Figure 3 around here>

Taken together, our findings confirm the existence of significant asymmetries in the dynamic relationship between the number of confirmed cases and deaths. More importantly, the continued presence of heterogeneity even after the large-scale vaccination implies that the underlying distributional differences in how the pandemic affects various segments of the population have not been eliminated. This further highlights the need for flexible and risk-sensitive public health policies that fully account for such heterogeneous effects in the post-vaccination phase.

5 Conclusion

This study exploits the QARDL methodology and examines the heterogeneous dynamic relationship between confirmed COVID-19 cases and deaths. Furthermore, we investigate the role of vaccination campaigns in shaping this relationship. Heterogeneity is assessed based on distributional differences in deaths across conditional quantiles. The empirical results reveal significant differences in the dynamic linkage between infection and mortality across different regions of the conditional death distribution. Despite persistent heterogeneity in fatality rates, vaccination campaigns have played a crucial role in reducing the fatality rate of COVID-19, with more pronounced effects observed in the upper tail of the conditional death distribution. These findings contribute to the existing literature that often overlooks heterogeneity for empirical analysis.

The current study also offers important implications for public health policymakers, highlighting the

need for targeted vaccination strategies and resource allocation to effectively protect vulnerable populations. The quantile-dependent empirical outcomes suggest that state-contingent strategies should be used in public health policies. The observed vaccination effect implies that timely vaccination and medical interventions substantially benefit mortality outcomes at the higher conditional percentile, suggesting that when the mortality outcomes are elevated, policymakers should prioritize vaccination coverage, booster deployment, and healthcare resources. In contrast, when the mortality outcomes are low, policies should focus more on disease monitoring, early detection, and preventive measures to stabilize short-run fluctuations without imposing excessive burdens on the healthcare system. Overall, the findings highlight that a one-size-fits-all policy may be inefficient, and adaptive, quantile-informed strategies can improve the effectiveness of the public health system. As the pandemic continues to evolve with the emergence of new variants and the potential decline of vaccine-induced immunity, further research is warranted to explore the long-term dynamics and refine policy interventions accordingly.

Although this study provides insights into the quantile-dependent dynamic relationship between confirmed COVID-19 cases and deaths, several directions remain for future research. First, future studies should incorporate variant-specific data to examine whether the heterogeneous effects identified in this study persist or change across different virus strains as new variants continue to emerge. Second, more detailed individual-level data, such as age, comorbidities, and vaccination status, can be employed to capture heterogeneity across demographic groups more efficiently. Finally, to conduct cross-country comparisons and assess the influence of different healthcare systems, public health interventions, and vaccination strategies on the short- and long-run relationships between confirmed cases and deaths, the QARDL framework can be extended to multi-country panel data.

References

Brodeur, A., D. Gray, A. Islam, and S. Bhuiyan. 2021. "A Literature Review of the Economics of COVID-19." *Journal of Economic Surveys* 35: 1007–1044.

Chang, B. H., R. Gohar, O. F. Derindag, and E. Uche. 2023. "COVID-19, Lockdown Measures and Their Impact on Food and Healthcare Prices: Empirical Evidence Using a Dynamic ARDL Model." *Journal of Economic Studies* 50: 1008–1026.

Chen, Y.-F., X. Ma, K. Sundell, K. Alaka, K. Schuh, J. Raskin, and R. A. Dean. 2016. "Quantile Regression

to Characterize Solanezumab Effects in Alzheimer's Disease Trials." *Alzheimer's & Dementia: Translational Research & Clinical Interventions* 2: 192–198.

Cho, J. S., T.-H. Kim, and Y. Shin. 2015. "Quantile Cointegration in the Autoregressive Distributed-Lag Modeling Framework." *Journal of Econometrics* 188: 281–300.

Deb, P., D. Furceri, D. Jimenez, S. Kothari, J. D. Ostry, and N. Tawk. 2022a. "The Effects of COVID-19 Vaccines on Economic Activity." *Swiss Journal of Economics and Statistics* 158: 1–25.

Deb, P., D. Furceri, J. D. Ostry, and N. Tawk. 2022b. "The Economic Effects of COVID-19 Containment Measures." *Open Economies Review* 33: 1–32.

Di Porto, E., P. Naticchioni, and V. Scrutinio. 2022. "Lockdown, Essential Sectors, and Covid-19: Lessons from Italy." *Journal of Health Economics* 81: 102572.

Fang, H., L. Wang, and Y. Yang. 2020. "Human Mobility Restrictions and the Spread of the Novel Coronavirus (2019-nCoV) in China." *Journal of Public Economics* 191: 104272.

Forsythe, S., J. Cohen, P. Neumann, S. M. Bertozzi, and A. Kinghorn. 2020. "The Economic and Public Health Imperatives around Making Potential Coronavirus Disease–2019 Treatments Available and Affordable." *Value in Health* 23:1427–1431.

Goel, R. K., J. R. Jones, and J. W. Saunoris. 2023. "Explaining Vaccine Hesitancy: A COVID-19 Study of the United States." *Managerial and Decision Economics* 44: 1073–1087.

Gupta, R. and S. K. Pal. 2020. "Trend Analysis and Forecasting of COVID-19 Outbreak in India." MedRxiv 2020–03.

Hammoudeh, S., W. Mensi, and J. S. Cho. 2022. "Spillovers between Exchange Rate Pressure and CDS Bid-Ask Spreads, Reserve Assets and Oil Prices Using the Quantile ARDL Model." *International Economics* 170: 66–78.

Hansen, N.-J. H. and R. C. Mano. 2023. "COVID-19 Vaccines: A Shot in the Arm for the Economy." *IMF Economic Review* 71: 148.

Hashmi, S. M., B. H. Chang, L. Huang, and E. Uche. 2022. "Revisiting the relationship between oil prices, exchange rate, and stock prices: An application of quantile ARDL model." *Resources Policy* 75: 102543.

Jeris, S. S. and R. D. Nath. 2020. "Covid-19, Oil Price and UK Economic Policy Uncertainty: Evidence from the ARDL Approach." *Quantitative Finance and Economics* 4: 503–514.

Jiang, F., Z. Zhao, and X. Shao. 2022. "Modelling the COVID-19 Infection Trajectory: A Piecewise Linear Quantile Trend Model." *Journal of the Royal Statistical Society Series B: Statistical Methodology* 84: 1589–1607.

Jin, R. 2021. "The Lag between Daily Reported Covid-19 Cases and Deaths and Its Relationship to Age." *Journal of Public Health Research* 10: 2049.

Jing, X. and J. S. Cho. 2025. "Forecasting the Confirmed COVID-19 Cases Using Modal Regression." *Journal of Forecasting* 44: 1578–1601.

Kim, D. and Y. J. Lee. 2022. "Vaccination Strategies and Transmission of COVID-19: Evidence across Advanced Countries." *Journal of Health Economics* 82: 102589.

Kountouris, Y. and K. Remoundou. 2024. "Education and Vaccine Hesitancy: Evidence from the COVID-19 Pandemic." *Economics Letters* 240: 111768.

Lee, K. and J. Hwang. 2025. "Impact of Underlying Diseases and Complications on COVID-19 Mortality in South Korea: Analysis of National Health Insurance Service Data." *Archives of Public Health* 83:20.

Liu, L., H. R. Moon, and F. Schorfheide. 2021. "Panel Forecasts of Country-Level Covid-19 Infections." *Journal of Econometrics* 220: 2–22.

McPhedran, R. and B. Toombs. 2021. "Efficacy or Delivery? An Online Discrete Choice Experiment to Explore Preferences for COVID-19 Vaccines in the UK." *Economics Letters* 200: 109747.

Mehta, N., S. Gupta, and S. Maitra. 2023. "House Prices and COVID-19 Pandemic Shocks in India: A Nonlinear ARDL Analysis." *International Journal of Housing Markets and Analysis* 16: 513–534.

Mori, M., A. Yokoyama, A. Shichida, K. Sasuga, T. Maekawa, and T. Moriyama. 2023. "Impact of Sex and Age on Vaccine-Related Side Effects and Their Progression after Booster mRNA COVID-19 Vaccine." *Scientific Reports* 13: 19328.

Okada, K. 2018. "Health and Political Regimes: Evidence from Quantile Regression." *Economic Systems* 42: 307–319.

O'Driscoll, M., G. Ribeiro Dos Santos, L. Wang, D. A. Cummings, A. S. Azman, J. Paireau, A. Fontanet, S. Cauchemez, and H. Salje. 2021. "Age-Specific Mortality and Immunity Patterns of SARS-CoV-2." *Nature* 590: 140–145.

Padula, W. V., S. Malaviya, N. M. Reid, B. G. Cohen, F. Chingcuanco, J. Ballreich, J. Tierce, and G. C. Alexander. 2021. "Economic Value of Vaccines to Address the COVID-19 Pandemic: A US Cost-Effectiveness and Budget Impact Analysis." *Journal of Medical Economics* 24: 1060–1069.

Rawlings, L., J. C. L. Looi, and S. J. Robson. 2022. "Economic Considerations in COVID-19 Vaccine Hesitancy and Refusal: A Survey of the Literature." *Economic Record* 98: 214–229.

Ribeiro, T. F., G. M. Cordeiro, F. A. Pena-Ramirez, and R. R. Guerra. 2021. "A New Quantile Regression for the COVID-19 Mortality Rates in the United States." *Computational and Applied Mathematics* 40: 255.

Silva, F. R., M. Simões, and J. S. Andrade. 2018. "Health Investments and Economic Growth: A Quantile Regression Approach." *International Journal of Development Issues* 17: 220–245.

Suah, J. L., M. Husin, P. S. K. Tok, B. H. Tng, T. Thevananthan, E. V. Low, M. R. Appannan, F. M. Zin, S. M. Zin, H. Yahaya, et al. 2022. "Waning COVID-19 Vaccine Effectiveness for BNT162b2 and CoronaVac in Malaysia: An Observational Study." *International Journal of Infectious Diseases*, 119, 69–76.

Sujath, R. a. a., J. M. Chatterjee, and A. E. Hassanien. 2020. "A Machine Learning Forecasting Model for COVID-19 Pandemic in India." *Stochastic Environmental Research and Risk Assessment* 34: 959–972.

Tan, M., P. T. Straughan, and G. Cheong. 2022. "Information Trust and COVID-19 Vaccine Hesitancy amongst Middle-Aged and Older Adults in Singapore: A Latent Class Analysis Approach." *Social Science & Medicine* 296: 114767.

Tiu, A., Z. Susswein, A. Merritt, and S. Bansal. 2022. "Characterizing the Spatiotemporal Heterogeneity of the COVID-19 Vaccination Landscape." *American Journal of Epidemiology* 191: 1792–1802.

Torres, C., J. García, F. Meslé, M. Barbieri, F. Bonnet, C. G. Camarda, E. Cambois, A. Caporali, É. Couppié, S. Poniakina, et al. 2023. "Identifying Age-and Sex-Specific COVID-19 Mortality Trends over Time in Six Countries." *International Journal of Infectious Diseases* 128: 32–40.

Ullah, A., T. Wang, and W. Yao. 2022. "Nonlinear Modal Regression for Dependent Data with Application

for Predicting COVID-19." *Journal of the Royal Statistical Society Series A: Statistics in Society* 185: 1424–1453.

Utami, A. M., F. Rendrayani, Q. A. Khoiry, D. Noviyanti, A. A. Suwantika, M. J. Postma, and N. Zakiyah. 2023. "Economic Evaluation of COVID-19 Vaccination: A Systematic Review." *Journal of Global Health* 13: 06001.

Verity, R., L. C. Okell, I. Dorigatti, P. Winskill, C. Whittaker, N. Imai, G. Cuomo-Dannenburg, H. Thompson, P. G. Walker, H. Fu, et al. 2020. "Estimates of the Severity of Coronavirus Disease 2019: A Model-Based Analysis." *The Lancet Infectious Diseases* 20: 669–677.

Variable	Mean	Median	Max	Min	Std. Dev.	Skewness	Kurtosis	n
Confirmed Cases	276.17	221.21	863.48	24.46	188.50	0.74	2.74	365
Deaths	4.00	3.18	14.96	0.30	3.01	0.94	3.13	365

Table 1: DESCRIPTIVE STATISTICS OF DAILY COVID-19 CONFIRMED CASES AND DEATHS IN THE UNITED STATES. This table reports descriptive statistics for daily new confirmed COVID-19 cases and deaths per million population in the United States from December 8, 2020 to December 7, 2021.

Variable	With Trend		Without Trend	
	Level	1st Difference	Level	1st Difference
Confirmed Cases	-1.6461	-19.0175***	-1.8829	-18.6542***
Deaths	-1.3483	-20.3265***	-1.4836	-20.2736***

Table 2: ADF TEST RESULTS FOR DAILY CONFIRMED COVID-19 CASES AND DEATHS. This table reports ADF unit root test statistics for daily confirmed COVID-19 cases and deaths in the United States over the period from December 8, 2020, to December 7, 2021. The tests are conducted under two specifications: with and without a deterministic trend, and for both level and first-differenced series. Lag lengths are selected based on the Bayesian information criterion. Notes: *, **, and *** indicate significance at 10%, 5%, and 1% significance levels, respectively.

τ	$\zeta_*(\tau)$	$\beta_*(\tau)$	$\lambda_*(\tau)$	$\delta_*(\tau)$
0.1	-0.3323***	0.0120***	-2.2685***	0.0093***
	(0.0243)	(0.0012)	(0.1546)	(0.0013)
0.2	-0.2544***	0.0126***	-2.5575***	0.009***
	(0.0227)	(0.0009)	(0.2603)	(0.0012)
0.3	-0.2405***	0.0126***	-3.0958***	0.0082***
	(0.0231)	(0.0007)	(0.3469)	(0.0015)
0.4	-0.2129***	0.0129***	-3.1513***	0.0082***
	(0.0239)	(0.0009)	(0.3741)	(0.0013)
0.5	-0.1788***	0.016***	-3.3311***	0.0078***
	(0.0197)	(0.0012)	(0.3586)	(0.0014)
0.6	-0.1646***	0.0186***	-3.5187***	0.0088***
	(0.0294)	(0.0018)	(0.2636)	(0.0018)
0.7	-0.1315***	0.0238***	-3.7000***	0.0097***
	(0.0242)	(0.0028)	(0.2610)	(0.0018)
0.8	-0.0966**	0.0278***	-3.5458***	0.0093***
	(0.0297)	(0.0065)	(0.2190)	(0.0017)
0.9	-0.0760***	0.0391***	-3.6006***	0.0104***
	(0.0190)	(0.0100)	(0.1986)	(0.0012)
Wald Tests				
p-values	0.0004	0.0001	0.0795	0.6576

Table 3: QARDL ESTIMATION RESULTS. (i) QARDL estimation results are based on the following model: $\Delta D_t = \alpha_*(\tau) + \zeta_*(\tau) D_{t-1} + \gamma_*(\tau) C_{t-1} + \sum_{j=1}^{p-1} \lambda_{j*}(\tau) \Delta D_{t-j} + \sum_{j=0}^{q-1} \delta_{j*}(\tau) \Delta C_{t-j} + U_t(\tau) = \alpha_*(\tau) + \zeta_*(\tau)(D_{t-1} - \beta_*(\tau) C_{t-1}) + \sum_{j=1}^{p-1} \lambda_{j*}(\tau) \Delta D_{t-j} + \sum_{j=0}^{q-1} \delta_{j*}(\tau) \Delta C_{t-j} + U_t(\tau)$. (ii) Standard errors are in parentheses, and those for the long-run coefficient are calculated using the delta method. (iii) The p-values of the Wald tests are computed to test the hypotheses: $H_0^{\zeta} : \zeta_*(0.25) = \zeta_*(0.5) = \zeta_*(0.75), H_0^{\beta} : \beta_*(0.25) = \beta_*(0.5) = \beta_*(0.75), H_0^{\lambda} : \lambda_*(0.25) = \lambda_*(0.5) = \lambda_*(0.75), H_0^{\delta} : \delta_*(0.25) = \delta_*(0.5) = \delta_*(0.75)$. (iv) * indicates a significance level of $p < 0.05$, ** indicates a significance level of $p < 0.01$, and *** indicates a significance level of $p < 0.001$.

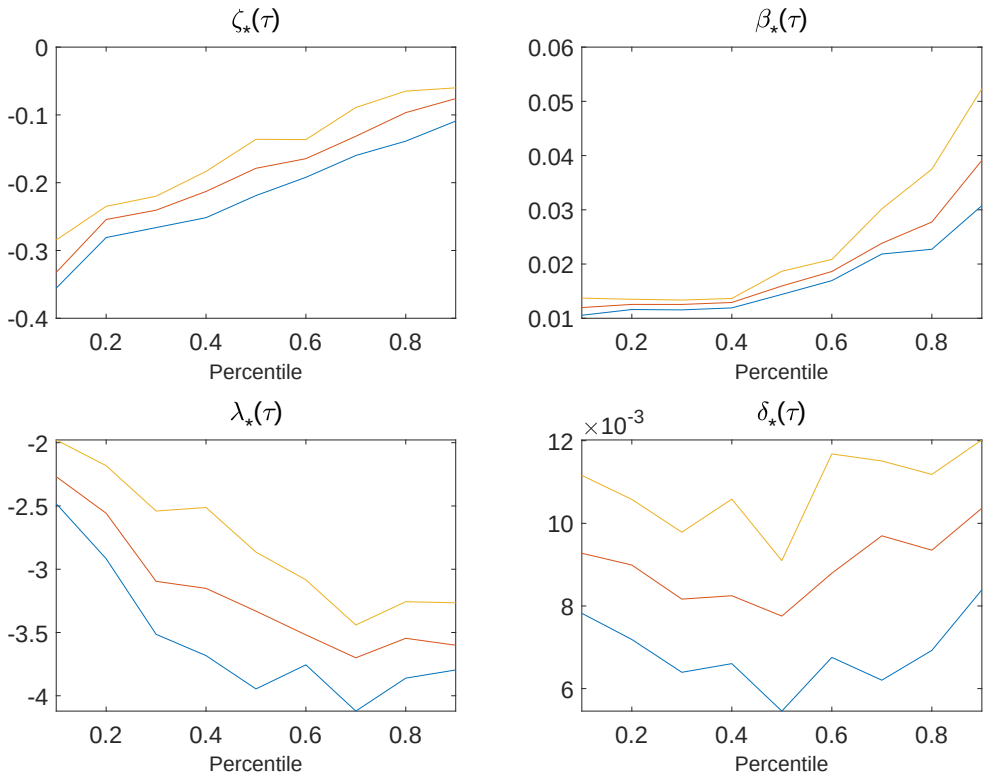

Figure 1: PARAMETER ESTIMATES USING THE WHOLE SAMPLE. The middle lines show the estimated parameters obtained by using all observations for different percentile levels: 0.1, 0.2, 0.3, 0.4, 0.5, 0.6, 0.7, 0.8, 0.9, along with 90% confidence bands.

Figure 2: PARAMETER ESTIMATES $\zeta_*(\tau)$, $\beta_*(\tau)$, $\lambda_*(\tau)$, AND $\delta_*(\tau)$ USING THE ROLLING WINDOW METHOD. The figures show the estimated parameters using the rolling window method with 90% confidence bands, and each window is constructed by 266 observations. Three different percentiles levels are employed: 0.25, 0.5, 0.75.

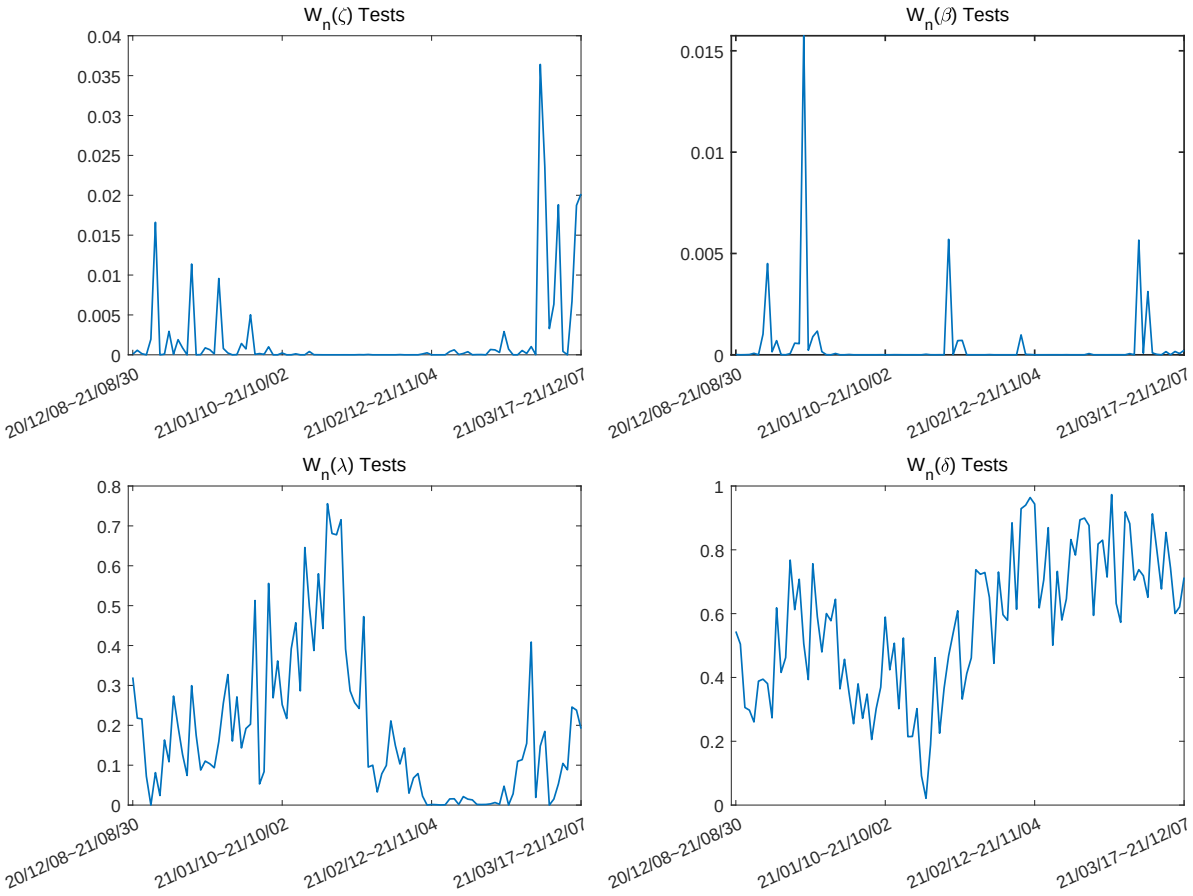

Figure 3: THE p-VALUES OF THE WALD TESTS. The figures show the estimated p-values of the Wald tests: (i) $\mathcal{W}_n(\beta)$ tests $H_0^\beta : \beta_*(0.25) = \beta_*(0.5) = \beta_*(0.75)$; (ii) $\mathcal{W}_n(\zeta)$ tests $H_0^\zeta : \zeta_*(0.25) = \zeta_*(0.5) = \zeta_*(0.75)$; (iii) $\mathcal{W}_n(\lambda)$ tests $H_0^\lambda : \lambda_*(0.25) = \lambda_*(0.5) = \lambda_*(0.75)$; and (iv) $\mathcal{W}_n(\delta)$ tests $H_0^\delta : \delta_*(0.25) = \delta_*(0.5) = \delta_*(0.75)$. The horizontal axis indicates the last observation of the window.